Li *et al. Journal of NeuroEngineering and Rehabilitation* (2024) 21:190
https://doi.org/10.1186/s12984-024-01488-6

Journal of NeuroEngineering and Rehabilitation

RESEARCH Open Access

Dynamical network-based evaluation for neuromuscular dysfunction in stroke-induced hemiplegia during standing

Jinping Li[1†], Na Zhang[2†], Ying Xu[1], Juan Wang[1], Xianglian Kang[3], Runing Ji[3], Ke Li[2*] and Ying Hou[1*]

Abstract

Background A given movement requires precise coordination of multiple muscles under the control of center nervous system. However, detailed knowledge about the changing characteristics of neuromuscular control for multi-muscle coordination in post-stroke hemiplegic patients during standing is still lacking. This study aimed to investigate the hemiplegia-linked neuromuscular dysfunction during standing from the perspective of multi-muscle dynamical coordination by utilizing a novel network approach – weighted recurrence network (WRN).

Methods Ten male hemiplegic patients with first-ever stroke and 10 age-matched healthy male adults were instructed to stand on a platform quietly for 30 s with eyes opened and eyes closed, respectively. The WRN was constructed based on the surface electromyography signals of 16 muscles from trunk, hips, thighs and calves. Relevant topological parameters, including clustering coefficient (*C*) and average shortest path length (*L*), were extracted to evaluate the dynamical coordination of multiple muscles. A measure of node centrality in network theory, degree of centrality (DC), was innovatively introduced to assess the contribution of single muscle in the multi-muscle dynamical coordination. The standing-related assessment metric, center of pressure (COP), was provided by the platform directly.

Results Results showed that the post-stroke hemiplegic patients stood with remarkably higher similarity of muscle activation and more coupled intermuscular dynamics, characterized by higher *C* and lower *L* than the healthy subjects ($p < 0.05$). The *DC* values and rankings of back, hip and calf muscles on the affected side were significantly decreased, whereas those on the unaffected side were significantly increased in hemiplegia group compared with the healthy group ($p < 0.05$). Without visual feedback, subjects exhibited enhanced muscle coordination and increased muscle involvement ($p < 0.05$). A decrease in *C* and an increase in *L* of WRN were observed with decreased COP areas ($p < 0.05$).

Conclusions These findings revealed that stroke-induced hemiplegia could significantly influence the neuromuscular control, which was manifested as more coupled intermuscular dynamics, abnormal deactivation of

[†]Jinping Li and Na Zhang contributed equally to this work.

*Correspondence:
Ke Li
kli@sdu.edu.cn
Ying Hou
horae1023@hotmail.com

Full list of author information is available at the end of the article

© The Author(s) 2024. **Open Access** This article is licensed under a Creative Commons Attribution-NonCommercial-NoDerivatives 4.0 International License, which permits any non-commercial use, sharing, distribution and reproduction in any medium or format, as long as you give appropriate credit to the original author(s) and the source, provide a link to the Creative Commons licence, and indicate if you modified the licensed material. You do not have permission under this licence to share adapted material derived from this article or parts of it. The images or other third party material in this article are included in the article's Creative Commons licence, unless indicated otherwise in a credit line to the material. If material is not included in the article's Creative Commons licence and your intended use is not permitted by statutory regulation or exceeds the permitted use, you will need to obtain permission directly from the copyright holder. To view a copy of this licence, visit http://creativecommons.org/licenses/by-nc-nd/4.0/.

muscles on affected side and compensation of muscles on unaffected side from the perspective of multi-muscle coordination. Enhanced multi-muscle dynamical coordination was strongly associated with impaired postural control. This study provides a novel analytical tool for evaluation of neuromuscular dysfunction and specification of responsible muscles for impaired postural control in stroke-induced hemiplegic patients, and could be potentially applied in clinical practice.

Keywords Stroke, Hemiplegia, Muscle networks, Neuromuscular dysfunction, Postural control, Surface electromyogram

Introduction

Postural control is a primary request of standing balance maintenance and is vulnerable to stroke. Post-stroke patients usually exhibit increased body sway, weight-bearing asymmetry, decreased limits of stability, body tilting and even falls [1–3]. The motor system, involving muscles, bones and joints, can generate a corrective, stabilizing torque to maintain the postural stability and orientation within the base of support [4]. To understand the mechanisms underlying postural control would help develop more indicators of motor functions relevant to impaired standing balance control and improve the efficiency of standing recovery after a stroke.

Postural control requires temporal and spatial coordination of multiple muscles. However, the damage to the pyramidal system and (or) extrapyramidal system in stroke survivors leads to interruption of descending motor paths and decreased common motoneuronal drives, ultimately manifesting as altered multi-muscle coordination [5, 6]. As one of the main motor behaviors for postural control, muscle synergies during walking has been studied in some depth. Asymmetric gait occurs after a stroke, as evidenced by differences in muscle synergies between sides. Compared with the affected side, muscle synergies related to unaffected side of hemiplegic patients were more similar to those of healthy individuals [7]. Besides, muscle synergies may merge after a stroke. It has been verified that fewer muscle synergies were needed to account for the whole muscle activity on the affected side when compared to the unaffected side [8], and rehabilitation training could significantly increase the number of muscle synergies during walking [9]. Upright standing can be approximated to a single inverted pendulum, with high demand on the coordination of muscles on trunk, hips, thighs and calves to counter gravity [10]. Surface electromyography (sEMG) studies in the standing position of post-stroke patients mainly focused on single-muscle activation and two-muscle coupling. Specifically, post-stroke patients have lower muscle activation and greater synchronous control between the antagonistic muscles on the affected lower limb [11, 12]. Stroke-related characteristics in muscle coordination during standing has been relatively less studied. Most of the research on muscle synergies during standing in post-stroke patients are generally combined with other tasks, such as reaching from standing, sit-to-stand transition and standing under disturbance [13–15]. The multi-muscle coordination of hemiplegic patients performing simple standing task is in urgent need of study.

Quantification of multi-muscle coordination relies on appropriate analytical tools. Previous studies about multi-muscle coordination are mostly based on non-negative matrix factorization (NMF), principal component analysis (PCA) and spectral coherence [6, 16, 17]. Tasks that are better analyzed by NMF and PCA are dynamic tasks, such as walking, running, pedaling and standing under perturbation [15, 18, 19]. These tasks satisfy the requirement of variation in activation amplitude for NMF and PCA to correctly identify synergy vectors of muscles [20–22]. When processing relatively steady sEMG signals, the role of NMF and PCA are very limited [23]. Besides, NMF and PCA are sensitive to the data length and signal quality of sEMG, thereby showing low robustness and repeatability in experimental studies [24]. Linear spectral coherence analysis assumes that a variety of muscles are coupled by linear relation, omitting the synchronizations between muscle complex. Therefore, some nonlinear analytical tools that are not based solely on signal amplitude and frequency variability, such as recurrence-based analysis, were proposed to assess the dynamical coordination of nonlinear, nonstationary neurophysiological signals [25, 26]. Recurrence-based analysis methods showed unique advantages in detection of the state changes in drifting dynamical motor systems and measurement of the rule-obeying structures in motor commands, especially for movements with little variation in sEMG signal amplitude [25–27]. By a careful choice of the setup parameters, recurrence-based analysis methods are relatively immune to noise [26]. However, these recurrence-based analysis methods had difficulty in describing detailed changes in specific muscles. In the examination of postural control during standing, there is a need to develop novel methods that can provide holistic and detailed information on intermuscular coordination.

Network analysis has its origins in graph theory and describes the spatiotemporal relationships between system elements through holistic and detailed characteristics, enabling in-depth exploration of the structure, behavior and function of systems [28, 29]. In the analysis of human electrophysiological signals, network analysis

has been widely used to characterize the organization of distributed brain activity [30]. In the last decade, muscle networks have been gaining attention and have provided powerful tools for monitoring the spatiotemporal synergetic relationships of multiple muscles [31–35]. Most of existing literature decodes functional muscle connectivity by linear spectral coherence and NMF [31, 33, 34, 36]. Recently, a novel multiplex recurrence network (MRN) approach has be proposed by combining dynamical recurrence with a multiplex network [37]. The MRN is suitable for the analysis of neurophysiological dynamics. It maps multivariate time series into phase space simultaneously to obtain trajectories and reveals the interactions of multiple subsystems through subtle recurrence features between trajectories, providing a new way to identify the structural and temporal characteristics of intermuscular dynamical coordination [25, 38]. In one of our previous studies, we employed the MRN to assess the intermuscular coordination for both grip and pinch at different force levels, and found that MRN could better explore the tiny changes of muscle coordination within a short time muscle contraction (less than 500 ms) compared with the NMF and PCA [39]. An intriguing issue is whether the MRN could provide insights into the intermuscular coordination of multiple muscles responsible for postural control and promote the evaluation of balance capacity for post-stroke patients.

Strongly shaped by the anatomical constraints of the musculoskeletal system and affected by tasks, the muscles of the functional network usually show unbalanced contributions [33]. Identifying the responsible muscles for abnormal coordinated actions may aid in developing more effective treatment programs of rehabilitation for patients with stroke. Using metrics that could measure the importance of nodes in the network, such as the degree of centrality (DC), the specific contributions of nodes in a network would be quantified and the abnormal function of nodes could be identified [40]. Unfortunately, little is known whether the contributions of multiple muscles involved in postural control during standing could be indexed, or the stroke-related impaired muscles could be identified.

The aim of this study was to evaluate the multi-muscle coordination for postural control during standing and to identify the abnormal muscle functions due to stroke. A weighted recurrence network (WRN) was constructed to analyze the dynamical coordination of multiple muscles responsible for standing balance. The DC was implemented to index the contributions of specific muscles in WRN. It was hypothesized that stroke would affect the dynamical coordination patterns for postural control, and it was also hypothesized that responsible muscles for impaired coordination after a stroke could be identified by using this novel method.

Methods

Subjects

Ten male hemiplegic patients and 10 healthy adults were recruited as the hemiplegia group and the control group, respectively. The inclusion criteria for post-stroke patients were as follows: (1) hemorrhagic or ischemic stroke confirmed by cranial computed tomography or magnetic resonance imaging; (2) first-ever stroke; (3) standing balance level II or III. The inclusion criteria for healthy adults were as follows: (1) gender and age matched to the patients; (2) neurologically intact. The exclusion criteria for all subjects were as follows: (1) post-stroke patients with lesion location in the cerebellum or brainstem; (2) history of lower extremity neurologic, musculoskeletal system diseases or injuries; (3) severe lumbar and cervical spine diseases; (4) lower extremity pain; (5) dizziness or vestibular system disorders; (6) recent use of medicine affecting balance control; (7) severe visual deficits. All participants gave their informed consent before the experiment. The characteristics of participants are listed in Table 1. The stroke type and lesion location of patients were determined with the help of brain imaging from the Department of Rehabilitation Medicine, Affiliated Suzhou Hospital of Nanjing Medical University. The affected side of post-stroke patients were more carefully confirmed by the professional therapists according to the lesion location and clinical symptoms. The study was performed with the approval of the Ethics Committee of Affiliated Suzhou Hospital of Nanjing Medical University according to the Declaration of Helsinki (K-2022-161-K01).

Experimental set-Up

Sixteen wireless sEMG electrodes (Trigno™, Delsys, USA) were placed on the muscle bellies of obliquus externus abdominis (OE), longissimus (LO), gluteus maximum (GMA), gluteus medius (GME), rectus femoris (RF), biceps femoris (BF), tibialis anterior (TA) and gastrocnemius caput mediale (GM) (Fig. 1a). The placement of electrodes followed the guidelines of the European SENIAM (surface EMG for non-invasive assessment of muscles) project [41]. For optimal sEMG signal recordings, the skin covering the target muscles were shaved, scrubbed and cleaned. All the 16-channel sEMG signals were synchronously recorded at 1926 Hz. The ProKin platform system (ProKin 254, TecnoBody, Italy) was applied to evaluate the bipedal stance static balance and measure the area of the center of pressure (COP).

Test protocol

Before the test, experimental staff placed four fixed locks beneath the balance board of the ProKin system and assisted the subjects in placing their foot on the prescribed position as instructed in the ProKin operating

Table 1 Characteristics of subjects

Number	Hemiplegia group									Control group		
	Age (y)	Height (cm)	Weight (kg)	Stroke type	Lesion location	Affected side	Months post-stroke	Level of standing balance	MMSE score	Age (y)	Height (cm)	Weight (kg)
1	56	163	75	Hemorrhagic	Left basal ganglia	Right	10.4	3	21	56	173	80
2	58	175	74	Hemorrhagic	Left basal ganglia	Right	7.3	3	8	63	169	60
3	39	168	82	Hemorrhagic	Left basal ganglia and temporal lobe	Right	3.7	2	25	34	173	83
4	41	173	80	Hemorrhagic	Left basal ganglia	Right	7.6	2	29	38	168	70
5	52	170	70	Hemorrhagic	Left basal ganglia	Right	5.7	2	11	57	170	69
6	61	172	75	Ischemic	Right lateral ventricle	Left	0.7	2	28	65	176	72
7	45	170	75	Hemorrhagic	Left basal ganglia	Right	3.4	3	29	51	175	75
8	68	170	75	Ischemic	Right basal ganglia	Left	1.1	3	26	65	160	73
9	43	169	92	Hemorrhagic	Left basal ganglia	Right	2.2	2	22	47	170	72
10	51	180	97	Hemorrhagic	Left basal ganglia	Right	4.9	2	23	56	167	53
Mean	51.4	171.0	79.5				4.7	2.4	22.2	53.2	170.1	70.7
SD	9.0	4.3	8.2				2.9	0.5	6.91	10.2	4.4	8.3

MMSE: Minimum Mental State Examination

manual: (1) the center axis of the feet is located on the A1 and A5 lines of the balance platform; (2) the highest points of the bilateral arches of the feet are located on the A3 and A5 lines of the balance platform; (3) the angle between the feet is 60 degrees; (4) the medial edges of the feet are 10 cm apart.

Subjects were instructed to stand still with both upper limbs hanging down naturally at the sides of the body and eyes looking straight ahead. During the standing test, the wireless sEMG system and the platform system were turned on synchronously to collect sEMG signals and assess bipedal static standing balance, respectively. Each subject was tested with two visual conditions – eye-opened (EO) and eye-closed (EC). For the EO test, subjects were instructed to stare at a 'marker' on the wall 1.5 m ahead for 30 s (Fig. 1b). For the EC test, the subjects' eyes were covered with a blindfold for 30 s. The EO and EC tests were repeated 3 times alternately. One min sitting break was provided between trials. All subjects successfully completed all tests.

Data analysis

For data pre-processing, the middle 20 s of 16-channel sEMG signals were retained. A fourth-order Butterworth band-pass filter at 20–500 Hz was applied to eliminate potential low-frequency noises and high-frequency interferences [42, 43]. A notch filter was used to remove the 50 Hz power line noise.

For m-channel sEMG signals $\{v(t)\}$, each channel of sEMG time series v could be reconstructed as a trajectory in high-dimensional phase space according to Taken's time delay theory [44]. The high-dimensional vector u of the trajectory can be constructed by the following formula:

$$u_i = [v_i, v_{i+\tau}, \ldots, v_{i+(d-1)\tau}] \tag{1}$$

Where $i = 1, 2, \ldots, N-(d-1)\tau$, and N is the length of the sEMG time series v. The time delay τ was set at 5 samples using mutual information [45], the embedding dimension d was set at 4 using false nearest neighbors [4, 45]. The spatial relationship between any two points i and j of the high-dimensional trajectory u could be represented by the adjacent matrix A:

$$A_{i,j} = \Theta\left(\varepsilon - \left\|u_i' - u_j'\right\|\right) - \delta \tag{2}$$

Where $\|\cdot\|$ is Euclidean distance, ε is a threshold value and was set at 80% of the maximum phase space radius according to experience [46], Θ is Heaviside function, and δ is Kronecker delta symbol. The value of $A_{i,j}$ equals to 1 if the distance between nodes i and j is less than or equal to ε, whereas the value of $A_{i,j}$ equals to 0 if the distance between nodes i and j is more than ε. Considering

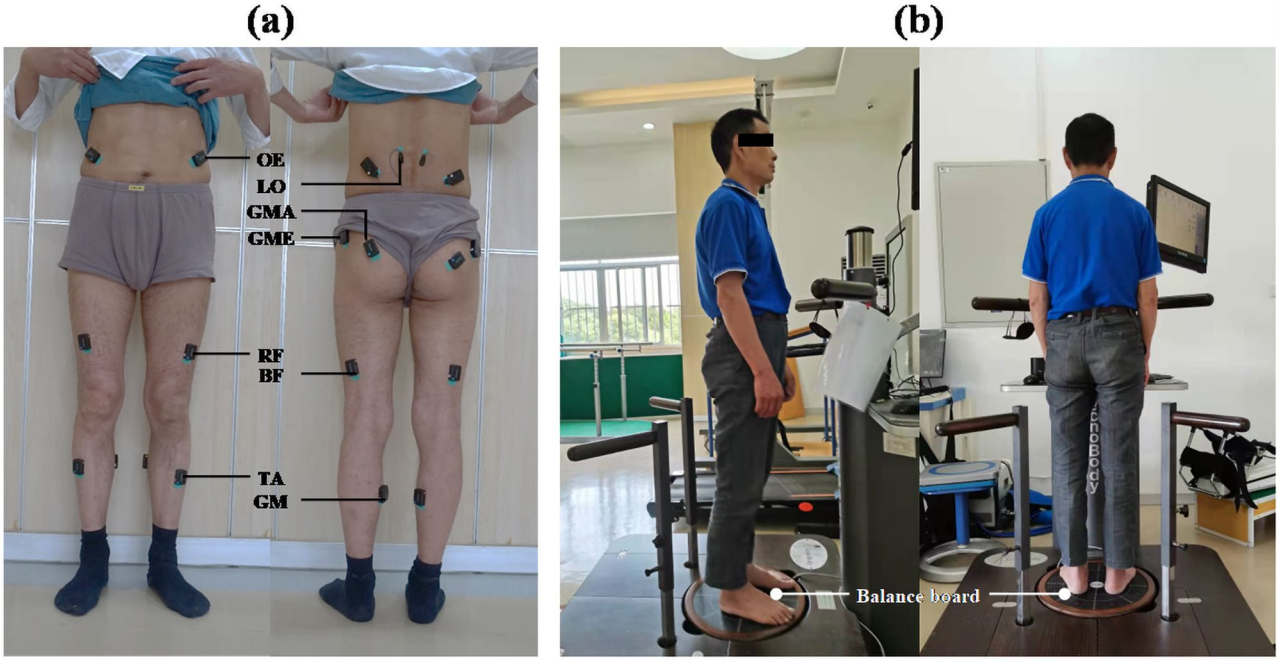

Fig. 1 Experimental set-up. (**a**) The positioning of sEMG electrodes; (**b**) The standing balance test

the adjacency matrix A of each sEMG time series as a binary network, there is a connection between nodes i and j if $A_{i,j} = 1$, whereas there is no connection between nodes i and j if $A_{i,j} = 0$.

The similarity of node degree distributions between two binary networks of each two sEMG times series could reflect the similarity of dynamical structure between two muscles' activation. In this study, the mutual information (I) was chosen to quantitatively measure the similarity of node degree distributions between binary networks of two muscles. Given a pair of muscles α and β, the I between the two muscles can be derived as:

$$I_{\alpha,\beta} = \sum_{k^{[\alpha]}} \sum_{k^{[\beta]}} P\left(k^{[\alpha]}, k^{[\beta]}\right) \log \frac{P\left(k^{[\alpha]}, k^{[\beta]}\right)}{P\left(k^{[\alpha]}\right) P\left(k^{[\beta]}\right)} \quad (3)$$

where $P\left(k^{[\alpha]}\right)$ and $P\left(k^{[\beta]}\right)$ are the degree distribution probabilities of binary networks A_α and A_β, respectively. The $P\left(k^{[\alpha]}, k^{[\beta]}\right)$ is the joint degree distribution probability of the existence of nodes with degree $k^{[\alpha]}$ in binary network A_α and $k^{[\beta]}$ in binary network A_β. The values of I are non-negative. Generally, the higher I represents higher similarity of the dynamical structures between two muscles' activation.

A m-node undirected WRN could be constructed by treating the muscles as nodes and the intermuscular I as the corresponding weights of the edges. In this study, the visualization threshold for WRN edges was empirically set to 60% of the maximum value of all network edge weights for all subjects. It was 0.45 in this study. Figure 2 illustrates the WRNs of representative subjects, including a post-stroke patient and a healthy adult. The affected and unaffected sides of the healthy controls were determined to be consistent with matched hemiplegic patients. For example, if the affected side of the hemiplegic patient was the left side, the left side of the matched control was defined as affected side and selected for subsequent comparison, and vice versa. Since there was no pathologically affected side in the healthy controls, we referred to the two sides of the control group as the matched-affected side and the matched-unaffected side, respectively.

The structural characteristics of WRN can be described by the clustering coefficient (C) and average shortest path length (L) as follows:

$$C = \frac{1}{m} \sum_{\alpha} \frac{1}{k_\alpha \left(k_\alpha - 1\right)} \sum_{\beta} \sum_{\gamma} \left(I_{\alpha,\beta} I_{\beta,\gamma} I_{\alpha,\gamma}\right)^{\frac{1}{3}} \quad (4)$$

where k_α is the degree of node α.

$$L = \sum_{\alpha,\beta \in V} \frac{d\left(\alpha,\beta\right)}{m\left(m-1\right)} \quad (5)$$

where V is the set of all nodes of WRN, $d(\alpha, \beta)$ is the weighted shortest path length between nodes α and β. The traditional C and L quantify the agglomeration of nodes and the efficiency of information flow in a network, respectively. Since the construction of WRN is based on the I of sEMG time series in this study, the C

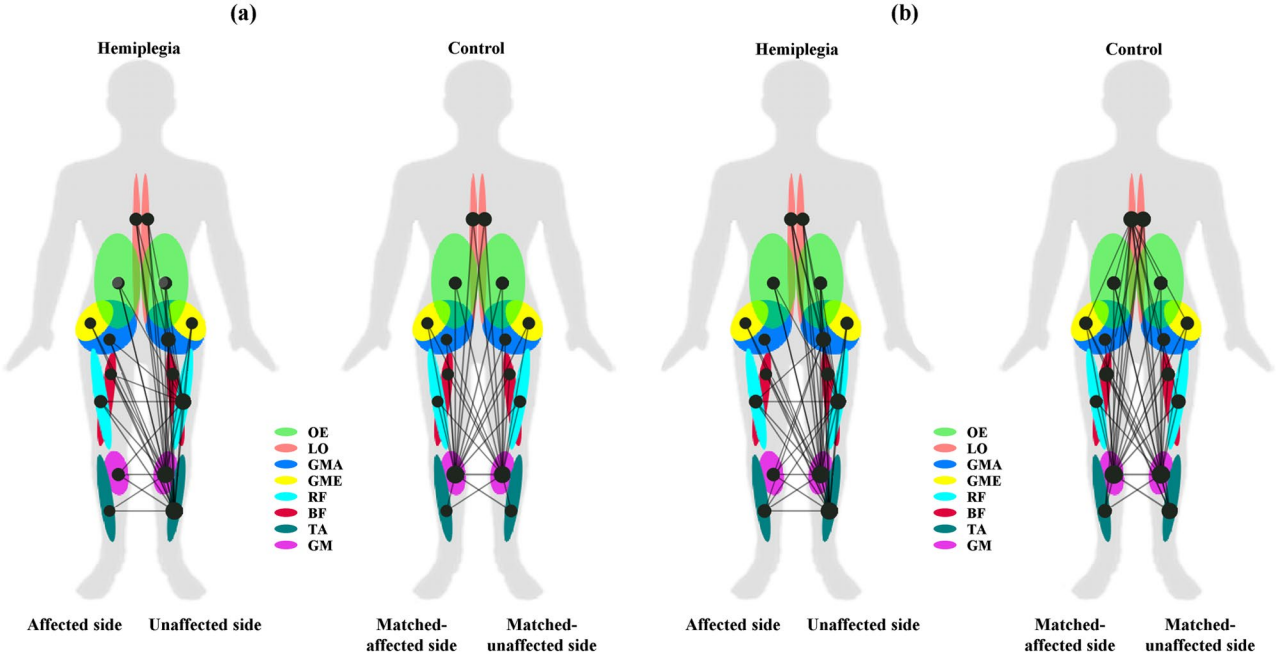

Fig. 2 Visualization of the WRN for representative subjects. (**a**) EO condition; (**b**) EC condition

and L are strongly related to the dynamical similarity and coupling of overall muscle activation, i.e. the higher C and the lower L, the higher similarity of muscle activation and the more coupled intermuscular dynamics.

In order to quantify the contribution of single muscle in the multi-muscle dynamical coordination, we introduced DC to the WRN. The DC of muscle α in the WRN is defined as:

$$DC_\alpha = \sum_{\beta \in V} w_{\alpha,\beta} \tag{6}$$

where $w_{\alpha,\beta}$ is the weight of edge between nodes α and β. Here, it equals to $I_{\alpha,\beta}$. According to this formula, the DC values are closely associated with the weights of edges. In order to minimize the effects of weights of edges on DC values and avoid erroneous results from directly comparing the DC values of different networks, we normalized the DC values into the range from 0 to 1 in a way that the original DC values of all nodes in one WRN were divided by the maximum DC value of the same WRN.

The sEMG data for each trial were segmented through a sliding window with a size of 1000 sample points and an overlap of 250 sample points. The segmented data were used to build the WRN and to extract the network parameters. In this study, we constructed the WRN from all 16-channel sEMG signals. The average of network parameters obtained from all sliding windows was taken as the result of one trial, and the average of network parameters from 3 trials under same test condition was used as the final result for that subject. The adjacency matrix A of single-channel sEMG signal was constructed using cross-recurrence plot toolbox 5.1 (MATLAB R2020a, The Mathworks, Natick, MA, USA). The area of COP was extracted directly from the bipedal stance static balance report provided by the ProKin system without additional calculation.

Statistical analysis

The statistical analyses were performed by SPSS 26.0 (SPSS Inc., Chicago, USA). A Shapiro-Wilk test was applied to verify the normal distribution of the data. For C and L of WRN, a two-way repeated measures ANOVA was applied to examine the effects of *group* and *vision*. A three-way repeated measures ANOVA was performed to evaluate the effects of *group*, *side* and *vision* on the normalized DC values of all muscle. Post hoc tests with the Bonferroni were used for all pairwise comparisons. A Pearson correlation analysis was utilized to analyze the correlations between holistic topological parameters of WRN and the area of COP. A p-value less than 0.05 was considered to be statistically significant.

Results

The functional connections of WRN of representative subjects were illustrated in Fig. 2. The functional muscle networks of representative hemiplegic patient showed more severe edge asymmetry between the affected and unaffected sides. Compared with the affected side, the post-stroke patient had more high-weighted connections between muscles on the unaffected side in both EO and EC conditions (Fig. 2). By contrast, the representative

healthy adult showed relatively symmetric network connections (Fig. 2). Visual conditions can affect the functional muscle networks. Removing the visual feedback increased the number and weight of edges in both hemiplegic patient and healthy adult, as can be observed from the fact that both the number and thickness of links in the WRN were greater in the EC condition than in the EO condition (Fig. 2).

Quantifications of WRN parameters for both groups under different visual conditions are presented in Fig. 3. The interaction effect of *group*×*vision* was found on clustering coefficient C ($F_{1,18}$ = 6.032, p=0.024), whereas the main effects of *group* and *vision* were found on average shortest path length L (groups: $F_{1,18}$ = 4.747, p=0.043; visual conditions: $F_{1,18}$ = 24.220, p<0.001). Compared with the healthy subjects, the post-stroke patients showed significantly higher C and lower L only for the EC condition (C: p=0.048; L: p=0.032). No significant difference was found in C (p=0.480) or L (p=0.081) between the two groups under the EO condition. Removal of visual feedback could lead to an increase in C and a decrease in L for the hemiplegia group (C: p=0.007; L: p=0.001), and a decrease in L for the control group (p=0.008). More information of ANOVA statistical results is listed in Additional file 1.

The three-way ANOVA test for normalized *DC* values of WRN were given in Table 2. The interaction of *group*, *side* and *vision* had a statistically significant effect only on the normalized DC values of OE and LO (OE: $F_{1,18}$ = 8.496, p=0.009; LO: $F_{1,18}$ = 8.769, p=0.008). An interaction effect between *group* and *side* was observed on the GMA, GME, TA and GM (GMA: $F_{1,18}$ = 4.901, p=0.040; GME: $F_{1,18}$ = 12.230, p=0.003; TA: $F_{1,18}$ = 12.189, p=0.003; GM: $F_{1,18}$ = 16.718, p=0.001). The interaction effect between *group* and *vision* was observed on the GME and TA (GME: $F_{1,18}$ = 5.767, p=0.027; TA: $F_{1,18}$ = 6.823, p=0.018). A significant difference between the patients and controls was observed in the normalized *DC* values of GMA and GM (GMA: $F_{1,18}$ = 5.575, p=0.030; GM: $F_{1,18}$ = 8.988, p=0.008). The main effect of *side* was observed on muscles BF, TA and GM, indicating a significant effect of *side* on the normalized *DC* values of BF, TA and GM (BF: $F_{1,18}$ = 10.361, p=0.005; TA: $F_{1,18}$ = 6.216, p=0.023; GM: $F_{1,18}$ = 7.327, p=0.014). An effect of *vision* was found on the normalized *DC* values of TA and GM (TA: $F_{1,18}$ = 10.604, p=0.004; GM: $F_{1,18}$ = 19.905, p<0.001). Specifically, the normalized *DC* values of GMA and TA on the unaffected side of hemiplegia group were significantly higher than those of control group (GMA: p=0.011; TA: p<0.001). In hemiplegia group, the normalized *DC* values of GMA, GME, TA and GM on the affected side were significantly lower than those on the unaffected side (GMA: p=0.016; GME: p=0.002; TA: p=0.001; GM: p<0.001), and the normalized *DC* values of TA and GM under the EC condition were significantly higher than those under the EO condition (TA: p=0.004; GM: p<0.01). However, neither *side* nor *vision* differences were found in the control group (p>0.05). More information of ANOVA statistical results is listed in Additional file 1.

The normalized *DC*s ranked in the descending order are shown in Fig. 4. The upper left and right panels show the *DC* ranking of the two groups under the EO and EC conditions, respectively. The ranking differences of the same muscles between the affected and unaffected sides were specified with the lines. In hemiplegia group, muscles on the unaffected side were positioned in higher rankings, while those on the affected side were positioned in relatively lower rankings. There were large side-differences in ranking positions between the bilateral LO, GMA, GME, TA and GM (Fig. 4a and b). Changes in the position of the same muscles in hemiplegia group compared to the control group are shown in the lower panels of Fig. 4. Compared to healthy individuals, the rankings of LO, GME, TA and GM on the affected side in stroke survivors dropped to lower positions under EO condition. Conversely, the rankings of GMA and TA on the unaffected side rose to higher positions (Fig. 4c). The EC condition showed similar results, expect for the GME that showed an increase of ranking (Fig. 4d).

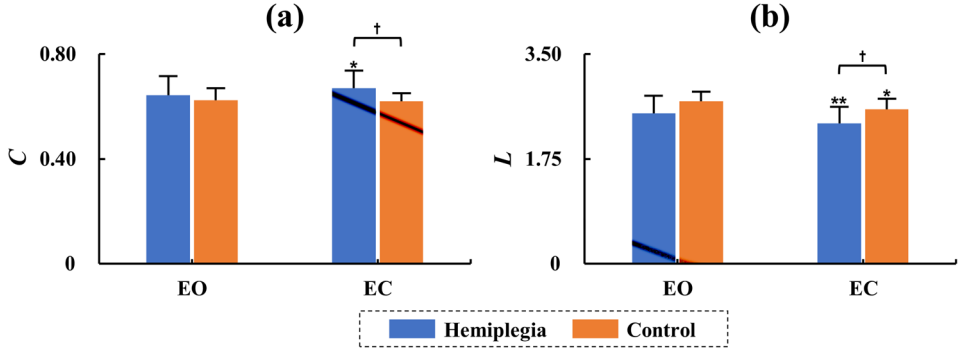

Fig. 3 Statistical results of functional muscle networks WRN. (a) Statistical results of parameter C; (b) Statistical results of parameter L. † (p < 0.05) significant difference between hemiplegia and control groups. * (p < 0.05) and ** (p < 0.001) significant differences between EO and EC conditions

Table 2 Summary table for three-way ANOVA of *group*, *side* and *vision* on normalized DC values (mean ± SD)

Muscles	Group	EO condition		EC condition		Main effect			Interaction effect			
		Affected side/Matched-affected side	Unaffected side/Matched-unaffected side	Affected side/Matched-affected side	Unaffected side/Matched-unaffected side	*Group*	*Side*	*Vision*	*Group×side*	*Group×vision*	*Side×vision*	*Group×side×vision*
OE	Hemiplegia	0.74 ± 0.08	0.73 ± 0.07	0.75 ± 0.07	0.76 ± 0.08	$p = 0.240$	$p = 0.400$	$p = 0.742$	$p = 0.324$	$p = 0.077$	$p = 0.519$	**$p = 0.009$**
	Control	0.70 ± 0.04	0.73 ± 0.10	0.70 ± 0.05	0.71 ± 0.09	$F = 1.480$	$F = 0.742$	$F = 0.112$	$F = 1.029$	$F = 3.522$	$F = 0.433$	**$F = 8.496$**
LO	Hemiplegia	0.73 ± 0.08	0.77 ± 0.06	0.75 ± 0.06	0.78 ± 0.06	$p = 0.480$	$p = 0.373$	$p = 0.286$	$p = 0.161$	$p = 0.362$	$p = 0.329$	**$p = 0.008$**
	Control	0.79 ± 0.07	0.77 ± 0.07	0.78 ± 0.06	0.78 ± 0.06	$F = 0.519$	$F = 0.836$	$F = 1.207$	$F = 2.135$	$F = 0.875$	$F = 1.006$	**$F = 8.769$**
GMA	Hemiplegia	0.72 ± 0.10	0.77 ± 0.09	0.73 ± 0.09	0.78 ± 0.09	**$p = 0.030$**	$p = 0.144$	$p = 0.969$	**$p = 0.040$**	$p = 0.064$	$p = 0.992$	$p = 0.781$
	Control	0.69 ± 0.08	0.68 ± 0.06	0.67 ± 0.07	0.66 ± 0.04	**$F = 5.575$**	$F = 2.328$	$F = 0.002$	**$F = 4.901$**	$F = 3.892$	$F < 0.001$	$F = 0.080$
GME	Hemiplegia	0.69 ± 0.10	0.74 ± 0.10	0.71 ± 0.10	0.76 ± 0.09	$p = 0.534$	$p = 0.097$	$p = 0.400$	**$p = 0.003$**	**$p = 0.027$**	$p = 0.561$	$p = 0.443$
	Control	0.72 ± 0.06	0.70 ± 0.07	0.71 ± 0.05	0.69 ± 0.05	$F = 0.403$	$F = 3.057$	$F = 0.743$	**$F = 12.230$**	**$F = 5.767$**	$F = 0.351$	$F = 0.615$
RF	Hemiplegia	0.74 ± 0.11	0.73 ± 0.11	0.75 ± 0.10	0.76 ± 0.08	$p = 0.200$	$p = 0.557$	$p = 0.145$	$p = 0.687$	$p = 0.268$	$p = 0.333$	$p = 0.088$
	Control	0.71 ± 0.07	0.69 ± 0.06	0.71 ± 0.06	0.69 ± 0.06	$F = 1.768$	$F = 0.359$	$F = 2.326$	$F = 0.168$	$F = 1.305$	$F = 0.992$	$F = 3.265$
BF	Hemiplegia	0.78 ± 0.12	0.85 ± 0.06	0.78 ± 0.10	0.85 ± 0.07	$p = 0.199$	**$p = 0.005$**	$p = 0.408$	$p = 0.696$	$p = 0.510$	$p = 0.380$	$p = 0.304$
	Control	0.72 ± 0.05	0.80 ± 0.11	0.77 ± 0.09	0.80 ± 0.11	$F = 1.777$	**$F = 10.361$**	$F = 0.717$	$F = 0.158$	$F = 0.453$	$F = 0.810$	$F = 1.120$
TA	Hemiplegia	0.68 ± 0.08	0.79 ± 0.09	0.74 ± 0.08	0.88 ± 0.06	$p = 0.103$	**$p = 0.023$**	**$p = 0.004$**	**$p = 0.003$**	**$p = 0.018$**	$p = 0.569$	$p = 0.331$
	Control	0.74 ± 0.10	0.72 ± 0.06	0.75 ± 0.09	0.73 ± 0.05	$F = 2.945$	**$F = 6.216$**	**$F = 10.604$**	**$F = 12.189$**	**$F = 6.823$**	$F = 0.336$	$F = 0.996$
GM	Hemiplegia	0.77 ± 0.10	0.92 ± 0.06	0.78 ± 0.09	0.93 ± 0.05	**$p = 0.008$**	**$p = 0.014$**	**$p < 0.001$**	**$p = 0.001$**	$p = 0.350$	$p = 0.320$	$p = 0.410$
	Control	0.90 ± 0.06	0.89 ± 0.06	0.93 ± 0.05	0.90 ± 0.07	**$F = 8.988$**	**$F = 7.327$**	**$F = 19.905$**	**$F = 16.718$**	$F = 0.920$	$F = 1.048$	$F = 0.712$

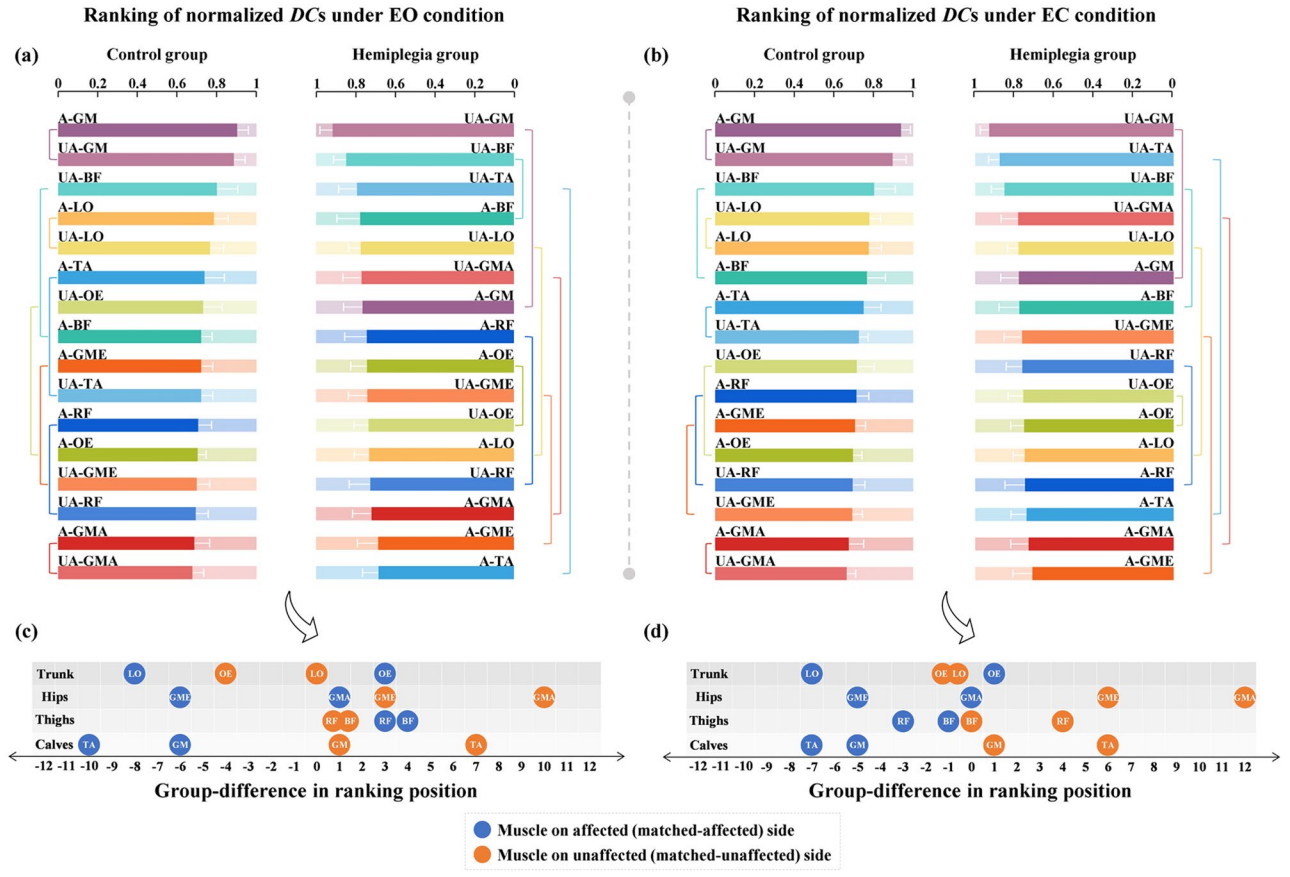

Fig. 4 The ranking of normalized *DC*s in descending order. (**a**) and (**b**) are the ranking of normalized *DC*s under EO and EC conditions, respectively. In hemiplegia group, A and UA represent the affected and unaffected sides, respectively; In control group, A and UA represent the matched-affected and matched-unaffected sides, respectively. The lines beside the bars represent the ranking differences of the same muscles between the affected (matched-affected) and unaffected (matched-unaffected) sides in one group. (**c**) and (**d**) are the ranking position changes of same muscles between hemiplegia and control group. Negative values represent a decrease in the *DC* ranking position of the muscle in hemiplegia group compared to the control group, while positive values represent an increase in the *DC* ranking position of the muscle in hemiplegia group compared to the control group

Figure 5 demonstrates the correlations between holistic topological parameters of WRN and area of COP. There were significant correlations between outcome measures of WRN and area of COP during standing. Regardless of EO or EC conditions, the *C* was significantly positively correlated with the area of COP (Fig. 5a, EO condition: $p=0.013$; EC condition: $p=0.033$), whereas the *L* was significantly negatively correlated with the area of COP (Fig. 5b, EO condition: $p=0.004$; EC condition: $p=0.013$).

Discussion

This study investigated the neuromuscular dysfunction related to stroke-induced hemiplegia during quiet standing. Changes in the multi-muscle dynamical coordination was examined using an advanced dynamical network analytical tool – WRN, which was built on the recurrence matrix of multi-channel sEMG signals. Results showed that the post-stroke patients had more severe asymmetry of functional muscle connectivity between the affected and unaffected sides than the healthy adults (Fig. 2). In addition, the patients showed remarkably higher *C* and lower *L*, implying higher similarity with more coupled intermuscular dynamics than the healthy subjects (Fig. 3). Patients with hemiplegia relied more on their unaffected side for postural control, which can be observed from the greater role played by muscles on that side in the overall muscle coordination (Table 2; Fig. 4). Significant differences of the WRN parameters between the patients and controls were more observable under the condition without visual feedback, suggesting that the absence of vision severely interfered with postural control in hemiplegic patients (Fig. 3; Table 2). Enhanced inter-muscular coordination was strongly associated with impaired balance control (Fig. 5).

Individuals with hemiplegia exhibited increased *C* and decreased *L* than the healthy subjects, which may suggest that the stroke survivors had higher similarity of muscle activation and more coupled intermuscular dynamics for maintaining standing balance. These results are in line with the previous findings that the

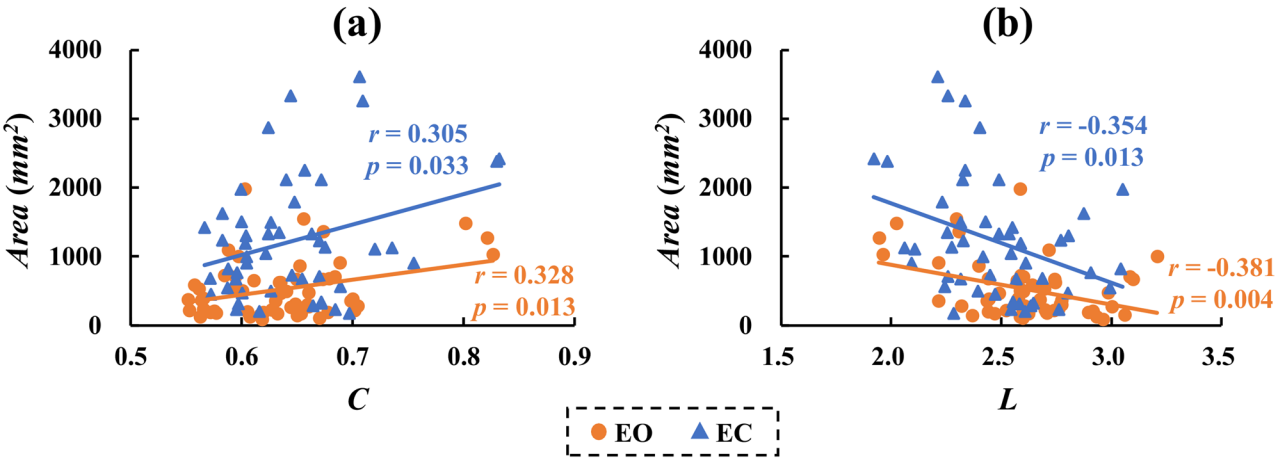

Fig. 5 The correlations between holistic topological parameters of WRN and area of COP. (a) Correlations between parameter *C* and area of COP; (b) Correlations between parameter *L* and area of COP

post-stroke individuals usually show augmented coupling during multiple muscle co-contraction [47, 48]. In the intact healthy adults, the central nervous system allows relatively independence and flexibility for different muscles during joint activation. But with stroke, the mechanism for independent and flexible motor control would be extensively confined [49]. Previous studies have reported that pathological conditions in neuromuscular system may reduce the dynamical degrees of freedom, which may limit the flexibility of motor system [4, 48]. Consistent with these findings, the current study further showed increased similarity and augmented dynamical coupling for muscle co-activation in hemiplegic patients, which may lead to a reduction in online adjustment of postures in according to the environment information [4]. This limitation in motor diversity and flexibility may ultimately result in maladaptive movement patterns and thus increase the risk of falls in stroke survivors. In clinic, Brunnstrom stages of stroke recovery, a scale including 6 phases of motor development and reorganization of the brain after a stroke, has been generally used to assess severity of comprehensive motor dysfunction [50]. The newly dynamical network-based approach in the present study may be more sensitive and accurate to neuromuscular control. These properties make the WRN a potential assessment method for identifying subtle changes in motor dysfunction and differentiating treatment more efficiently.

Evaluating the contribution of each muscle in the functional muscle network would be a challenging issue. This study firstly introduced *DC* to the WRN to indicate the role of each muscle played in multiple muscle co-contraction. Results of *DC* revealed that the muscles on both affected and unaffected sides were influenced by the stroke, but the symptoms between sides were significant different. The normalized *DC* value of the GM on the affected side was significantly lower than that of the unaffected side and that of healthy adults. Meanwhile, the normalized *DC* values of the GMA, GME and TA on the unaffected side were significantly higher than those of the affected side and those of the healthy adults (Table 2). These results were further confirmed by the rankings of normalized *DC* values (Fig. 4). Compared to the healthy subjects, the LO, GME, TA and GM of affected side showed substantial drops of *DC* rankings, and the GMA, GME and TA of the unaffected side showed substantial increases of *DC* rankings (Fig. 4). These results also indirectly support the fact that the affected-side muscles possess more high-weighted connections, with asymmetric contributions across side in hemiplegic patients (Fig. 2). The asymmetric damage to cortical regions caused by stroke would be responsible for the inter-side differences in muscle coordination. Impaired abilities of sensory information integration and motor commands submission may also contribute the inconsistent *DC* rankings across sides [51]. In contrast to the ranking drops of muscles on the affected side, the muscles on unaffected side showed remarkable increase of *DC* rankings. This may corroborate the viewpoint that the muscles on unaffected side, especially the gluteal and calf muscles, receive more central regulation, perform greater activation, and make a more important contribution to the multi-muscle coordination when maintaining the upright posture [11, 52, 53]. In future treatment and rehabilitation, substitution of unaffected side muscles should be rationally removed or utilized. Conversely, the muscles with lower *DC* ranking on the affected side deserve more clinicians' consideration to improve their activation by administering rehabilitation training. It is noteworthy that the ranking of LO on the affected side was much lower than that of the healthy individuals, suggesting weakness, delayed activation and malfunction of the trunk-related muscles

in post-stroke patients [54, 55]. A potential use of *DC* and its ranking may facilitate the clinicians to quantify the importance of each involved muscles in a complex co-activation process and potentially identify the muscles responsible for motor dysfunction.

The functional muscle network parameters of WRN had significant correlations with the area of COP (Fig. 5). The area of COP is valid for assessing the ability of postural control [56]. As the *C* decreased and the *L* increased, there was a corresponding decrease in subjects' area of COP (Fig. 5). These changes suggested that good standing balance performance is strongly associated with a lower degree of intermuscular coordination. Pathologically enhanced muscle coordination would be one of the direct reasons for poor balance performance in hemiplegic patients. It is a reliable way to improve postural control by improving muscle coordination relationships. Besides, hemiplegic patients' balance ability and fall risk could be indirectly determined by functional muscle network parameters. When the results of functional muscle network parameters are outside the normal range, the subject may have insufficient postural control and higher fall risk.

This study further confirmed the role of vision in standing balance control. Removal of visual information could lead to enhanced muscle coupling and increased intermuscular similarity (Fig. 3). Previous studies reported that the allocentric, egocentric and geocentric spatial frames provided by the vision, somatosensory and vestibular system could facilitate the central nervous system to determine the orientation and state of body in environment, and thus make correct motion planning and suitable motor commands for balance control [57]. Without visual feedback, subjects may actively reduce the dynamical degrees of freedom, ultimately manifesting as increased intermuscular similarity, augmented muscle coupling and reduced motion flexibility [26].

Limitations

There are many limitations in our study. First, the number of subjects was relatively small and all subjects recruited were male adults. In subsequent studies, more subjects, including female adults, need to be recruited and grouped. Second, post-stroke patients were recruited without restriction of cognitive conditions. Although all patients completed the standing tasks, the quality of task completion may be lower in patients with cognitive impairment. Third, the determination matched-affected and matched-unaffected sides of the healthy controls were consistent with matched hemiplegic patients only according to anatomical structure. It is necessary to consider the dominant and non-dominant limbs in defining the matched-affected and matched-unaffected sides of the healthy control group. Fourth, the stroke recovery stages on intermuscular coordination during standing have not been studied. In future study, we would continuously follow the rehabilitation process of post-stroke patients, extract their muscle network parameters at different stages of disease duration, and correlate the network-extracted parameters with the patients' recovery stages. Fifth, concluding asymmetry of stroke patients based only on bilateral functional network connections and unbalanced muscle contributions lacks some scientific validity. It would be interesting to establish unilateral functional networks for the affected and unaffected sides and extract relevant parameters to quantitatively assess the asymmetry of muscle coordination after a stroke.

Conclusions

A novel analytical tool – WRN was proposed to investigate the stroke-induced neuromuscular dysfunction during standing from the perspective of multi-muscle dynamical coordination. Results revealed that stroke-induced hemiplegia could significantly influence the neuromuscular control, as evidenced by more coupled intermuscular dynamics, abnormal deactivation of muscles on affected side and compensation of muscles on unaffected side from the perspective of multi-muscle coordination. Enhanced multi-muscle dynamical coordination was strongly associated with impaired postural control. The WRN and related parameters could be used in evaluation of neuromuscular dysfunction and identifying the responsible muscles for impaired postural control in post-stroke patients.

Abbreviations

sEMG	Surface electromyography
NMF	Non-negative matrix factorization
PCA	Principal component analysis
MRN	Multiplex recurrence network
DC	Degree of centrality
WRN	Weighted recurrence network
OE	Obliquus externus abdominis muscle
LO	Longissimus muscle
GMA	Gluteus maximum muscle
GME	Gluteus medius muscle
RF	Rectus femoris muscle
BF	Biceps femoris muscle
TA	Tibialis anterior muscle
GM	Gastrocnemius caput mediale muscle
COP	Center of pressure
EO	Eyes opened
EC	Eyes closed
I	Mutual information
C	Clustering coefficient
L	Average shortest path length

Supplementary Information

The online version contains supplementary material available at https://doi.org/10.1186/s12984-024-01488-6.

Supplementary Material 1

Acknowledgements
The authors thank all subjects for their participation in the experiment.

Author contributions
YH and KL conceived the idea. NZ, TT, YX and JW performed the experiments. YH, KL and RJ provided guidance and resources. JL, NZ and XK analyzed the results. JL wrote the original manuscript and prepared all figures. KL, YH and JL revised the manuscript. All authors edited the manuscript and approved the final manuscript.

Funding
This study was supported by the National Natural Science Foundation of China (62073195), the Key Research & Development Programs of Shandong Province (2019GSF108164, 2019GSF108127, 2019JZZY021010), the Key Disciplines Construction Project of Suzhou (SZXK201811), and Science and Technology Program of Suzhou (SKY2021053, SKY2022186).

Data availability
The datasets generated and/or analyzed in the current study are available from the corresponding author upon reasonable request.

Declarations

Ethics approval and consent to participate
The experimental procedures were approved by Ethics Committee of the Affiliated Suzhou Hospital of Nanjing Medical University (K-2022-161-K01) and were in accordance with the Declaration of Helsinki. All participants gave their informed consent before test.

Consent for publication
Participants give their consent for publication of their image.

Competing interests
The authors declare no competing interests.

Author details
[1]Department of Neurological Rehabilitation, Suzhou Municipal Hospital, The Affiliated Suzhou Hospital of Nanjing Medical University, Gusu School of Nanjing Medical University, Suzhou 215000, China
[2]Laboratory of Rehabilitation Engineering, Intelligent Medical Engineering Research Center, School of Control Science and Engineering, Shandong University, Jinan 250061, China
[3]Present address: Department of Medical Engineering, Suzhou Municipal Hospital, The Affiliated Suzhou Hospital of Nanjing Medical University, Gusu School of Nanjing Medical University, Suzhou 215000, China

Received: 17 December 2023 / Accepted: 11 October 2024
Published online: 24 October 2024

References

1. Pérennou D. Weight bearing asymmetry in standing hemiparetic patients. J Neurol Neurosurg Psychiatry. 2005;76(5):621.
2. Weerdesteyn V, Niet M, Duijnhoven H, Geurts A. Falls in individuals with stroke. J Rehabil Res Dev. 2008;45:1195–213.
3. Goldie P, Evans O, Matyas T. Performance in the stability limits test during rehabilitation following stroke. Gait Posture. 1996;4(4):315–22.
4. Li J, Zhang Y, Song S, Hou Y, Hong Y, Yue S, et al. Dynamical Analysis of Standing Balance Control on Sloped Surfaces in individuals with Lumbar Disc Herniation. Sci Rep. 2020;10(1):1676.
5. Neckel N, Pelliccio M, Nichols D, Hidler J. Quantification of functional weakness and abnormal synergy patterns in the lower limb of individuals with chronic stroke. J Neuroeng Rehabil. 2006;3(1):17.
6. Cheung VCK, Turolla A, Agostini M, Silvoni S, Bennis C, Kasi P, et al. Muscle synergy patterns as physiological markers of motor cortical damage. Proc Natl Acad Sci. 2012;109(36):14652–6.
7. Coscia M, Monaco V, Martelloni C, Rossi B, Chisari C, Micera S. Muscle synergies and spinal maps are sensitive to the asymmetry induced by a unilateral stroke. J Neuroeng Rehabil. 2015;12(1):39.
8. Barroso FO, Torricelli D, Molina-Rueda F, Alguacil-Diego IM, Cano-de-la-Cuerda R, Santos C, et al. Combining muscle synergies and biomechanical analysis to assess gait in stroke patients. J Biomech. 2017;63:98–103.
9. Ardestani MM, Kinnaird CR, Henderson CE, Hornby TG. Compensation or recovery? Altered kinetics and neuromuscular synergies following high-intensity stepping training Poststroke. Neurorehabil Neural Repair. 2019;33(1):47–58.
10. Danna-Dos-Santos A, Boonstra TW, Degani AM, Cardoso VS, Magalhaes AT, Mochizuki L, et al. Multi-muscle control during bipedal stance: an EMG–EMG analysis approach. Exp Brain Res. 2014;232(1):75–87.
11. Wang W, Xiao Y, Yue S, Wei N, Li K. Analysis of center of mass acceleration and muscle activation in hemiplegic paralysis during quiet standing. PLoS ONE. 2019;14(12):e0226944.
12. Yamanaka E, Goto R, Kawakami M, Tateishi T, Kondo K, Nojima I. Intermuscular coherence during quiet standing in Sub-acute patients after Stroke: an exploratory study. Brain Sci. 2023;13(12).
13. Tomita Y, Turpin NA, Piscitelli D, Feldman AG, Levin MF. Stability of reaching during standing in stroke. J Neurophysiol. 2020;123(5):1756–65.
14. Kogami H, An Q, Yang N, Wang R, Yoshida K, Hamada H, et al. Analysis of muscle synergy and kinematics in sit-to-stand motion of hemiplegic patients in subacute period. Adv Robot. 2021;35(13–14):867–77.
15. Torres-Oviedo G, Ting LH. Subject-specific muscle synergies in human balance control are consistent across different biomechanical contexts. J Neurophysiol. 2010;103(6):3084–98.
16. Laine CM, Valero-Cuevas FJ. Intermuscular coherence reflects functional coordination. J Neurophysiol. 2017;118(3):1775–83.
17. Sadeghi H, Prince F, Sadeghi S, Labelle H. Principal component analysis of the power developed in the flexion/extension muscles of the hip in able-bodied gait. Med Eng Phys. 2000;22(10):703–10.
18. Hug F, Turpin NA, Couturier A, Dorel S. Consistency of muscle synergies during pedaling across different mechanical constraints. J Neurophysiol. 2011;106(1):91–103.
19. Barroso FO, Torricelli D, Moreno JC, Taylor J, Gomez-Soriano J, Bravo-Esteban E, et al. Shared muscle synergies in human walking and cycling. J Neurophysiol. 2014;112(8):1984–98.
20. Oliveira AS, Gizzi L, Farina D, Kersting UG. Motor modules of human locomotion: influence of EMG averaging, concatenation, and number of step cycles. Front Hum Neurosci. 2014;8:335.
21. Steele KM, Tresch MC, Perreault EJ. Consequences of biomechanically constrained tasks in the design and interpretation of synergy analyses. J Neurophysiol. 2015;113(7):2102–13.
22. Ranganathan R, Krishnan C. Extracting synergies in gait: using EMG variability to evaluate control strategies. J Neurophysiol. 2012;108(5):1537–44.
23. Li J, Kang X, Li K, Xu Y, Wang Z, Zhang X, et al. Clinical significance of dynamical network indices of surface electromyography for reticular neuromuscular control assessment. J Neuroeng Rehabil. 2023;20(1):170.
24. Turpin NA, Uriac S, Dalleau G. How to improve the muscle synergy analysis methodology? Eur J Appl Physiol. 2021;121(4):1009–25.
25. Li K, Wei N, Cheng M, Hou X, Song J. Dynamical Coordination of Hand Intrinsic Muscles for Precision Grip in diabetes Mellitus. Sci Rep. 2018;8(1):4365.
26. Li J, Wei N, Yue S, Li K. Multidimensional recurrence quantification analysis of multi-muscle synergy in Elderly during standing on slopes. Annu Int Conf IEEE Eng Med Biol Soc. 2020;3114–7.
27. Zbilut JP, Thomasson N, Webber CL. Recurrence quantification analysis as a tool for nonlinear exploration of nonstationary cardiac signals. Med Eng Phys. 2002;24(1):53–60.
28. Boccaletti S, Latora V, Moreno Y, Chavez M, Hwang DU. Complex networks: structure and dynamics. Phys Rep. 2006;424(4–5):175–308.
29. Buzsáki G, Draguhn A. Neuronal oscillations in cortical networks. Science. 2004;304(5679):1926–9.
30. Bullmore E, Sporns O. Complex brain networks: graph theoretical analysis of structural and functional systems. Nat Rev Neurosci. 2009;10(3):186–98.
31. Boonstra TW, Danna-Dos-Santos A, Xie HB, Roerdink M, Stins JF, Breakspear M. Muscle networks: connectivity analysis of EMG activity during postural control. Sci Rep. 2015;5:17830.
32. Kerkman JN, Daffertshofer A, Gollo LL, Breakspear M, Boonstra TW. Functional connectivity analysis of multiplex muscle network across frequencies. Annu Int Conf IEEE Eng Med Biol Soc. 2017;1567–70.
33. Kerkman JN, Daffertshofer A, Gollo LL, Breakspear M, Boonstra TW. Network structure of the human musculoskeletal system shapes neural interactions on multiple time scales. Sci Adv. 2018;4(6):eaat0497.

34. Kerkman JN, Bekius A, Boonstra TW, Daffertshofer A, Dominici N. Muscle synergies and coherence networks reflect different modes of Coordination during walking. Front Physiol. 2020;11:751.
35. Houston M, Li X, Zhou P, Li S, Roh J, Zhang Y. Alterations in muscle networks in the Upper Extremity of Chronic Stroke survivors. IEEE Trans Neural Syst Rehabil Eng. 2021;29:1026–34.
36. Luo Y, Guo T, Wang R, Mu S, Tao K. Decoding invariant spatiotemporal synergy patterns on muscle networks of lower-limb movements via surface electromyographic signals. Biomed Signal Process Control. 2024;91:106033.
37. Eroglu D, Marwan N, Stebich M, Kurths J. Multiplex Recurrence Networks Phys Rev E. 2018;97:012312.
38. Lacasa L, Nicosia V, Latora V. Network structure of multivariate time series. Sci Rep. 2015;5:15508.
39. Zhang N, Li K, Li G, Nataraj R, Wei N. Multiplex Recurrence Network Analysis of Inter-muscular Coordination during Sustained grip and pinch contractions at different force levels. IEEE Trans Neural Syst Rehabil Eng. 2021;29:2055–66.
40. Freeman LC. Centrality in social networks conceptual clarification. Social Networks. 1978;1(3):215–39.
41. Stegeman D, Hermens H. Standards for suface electromyography: The European project Surface EMG for non-invasive assessment of muscles (SENIAM). 2007;1.
42. Luca CJD. The Use of Surface Electromyography in Biomechanics. J Appl Biomech. 1997;13:135–63.
43. De Luca CJ, Gilmore LD, Kuznetsov M, Roy SH. Filtering the surface EMG signal: Movement artifact and baseline noise contamination. J Biomech. 2010;43(8):1573–9.
44. Marwan N, Carmen Romano M, Thiel M, Kurths J. Recurrence plots for the analysis of complex systems. Phys Rep. 2007;438(5–6):237–329.
45. Marwan N, Webber CL. Mathematical and computational foundations of recurrence quantifications. In: Webber JCL, Marwan N, editors. Recurrence quantification analysis: Theory and Best practices. Cham: Springer International Publishing; 2015. pp. 3–43.
46. Li J, Hou Y, Wang J, Zheng H, Wu C, Zhang N et al. Functional muscle network in post-stroke patients during quiet Standing. Annu Int Conf IEEE Eng Med Biol Soc. 2021;874–7.
47. Hesam-Shariati N, Trinh T, Thompson-Butel AG, Shiner CT, McNulty PA. A longitudinal Electromyography Study of Complex movements in Poststroke Therapy. 2: changes in coordinated muscle activation. Front Neurol. 2017;8:277.
48. Santello M, Lang CE. Are movement disorders and sensorimotor injuries pathologic synergies? When normal multi-joint movement synergies become pathologic. Front Hum Neurosci. 2014;8:1050.
49. Yang Y, Yang M, Li H, Chen T, Liu Y, Liu B. Investigating the descending motor tracts in patients with chronic ischemic stroke with diffusion tensor imaging. Natl Med J China. 2015;95:1842–5.
50. Brunnstrom S. Motor Testing procedures in Hemiplegia: based on sequential recovery stages. Phys Ther. 1966;46(4):357–75.
51. Farmer SF, Swash M, Ingram DA, Stephens JA. Changes in motor unit synchronization following central nervous lesions in man. J Physiol. 1993;463:83–105.
52. Cheng PT, Chen C-L, Wang C-M, Hong W-H. Leg Muscle Activation Patterns of Sit-to-Stand Movement in Stroke patients. Am J Phys Med Rehabil. 2004;83:10–6.
53. Prudente C, Rodrigues-de-Paula F, Faria CD. Lower limb muscle activation during the sit-to-stand task in subjects who have had a stroke. Am J Phys Med Rehabil. 2013;92(8):666–75.
54. Bohannon RW. Measurement of trunk muscle strength after stroke: an integrative review. Top Stroke Rehabil. 2022;29(3):173–80.
55. Bohannon RW, Cassidy D, Walsh S. Trunk muscle strength is impaired multidirectionally after stroke. Clin Rehabil. 1995;9(1):47–51.
56. Hasan SS, Robin DW, Szurkus DC, Ashmead DH, Peterson SW, Shiavi RG. Simultaneous measurement of body center of pressure and center of gravity during upright stance. Part I: methods. Gait Posture. 1996;4(1):1–10.
57. Peterka RJ. Chapter 2 - sensory integration for human balance control. Handbook of clinical neurology. Volume 159. Elsevier; 2018. pp. 27–42.

Publisher's note

Springer Nature remains neutral with regard to jurisdictional claims in published maps and institutional affiliations.